0026-895X/05/6802-305–316$20.00
MOLECULAR PHARMACOLOGY
Vol. 68, No. 2
9506/3042849
Mol Pharmacol 68:305–316, 2005
Printed in U.S.A.

A Single Residue in the S6 Transmembrane Domain Governs the Differential Flecainide Sensitivity of Voltage-Gated Potassium Channels

Daniel Herrera, Aida Mamarbachi, Manuel Simoes, Lucie Parent, Rémy Sauvé, Zhiguo Wang, and Stanley Nattel

Montreal Heart Institute and Department of Medicine (D.H., A.M., Z.W., S.N.), and Departments of Pharmacology (D.H.) and Physiology (M.S., L.P., R.S.), University of Montreal, Montreal, Quebec, Canada; and Department of Pharmacology and Therapeutics, McGill University, Montreal, Quebec, Canada (S.N.)

Received November 22, 2004; accepted May 9, 2005

ABSTRACT

Flecainide has been used to differentiate Kv4.2-based transient-outward K^+-currents (flecainide-sensitive) from Kv1.4-based (flecainide-insensitive). We found that flecainide also inhibits ultrarapid delayed rectifier (I_{Kur}) currents in *Xenopus laevis* oocytes carried by Kv3.1 subunits (IC_{50}, 28.3 ± 1.3 μM) more strongly than Kv1.5 currents corresponding to human I_{Kur} (IC_{50}, 237.1 ± 6.2 μM). The present study examined molecular motifs underlying differential flecainide sensitivity. An initial chimeric approach pointed to a role for S6 and/or carboxyl-terminal sites in Kv3.1/Kv1.5 sensitivity differences. We then looked for homologous amino acid residues of the two sensitive subunits (Kv4.2 and Kv3.1) different from homologous residues for insensitive subunits (Kv1.4 and Kv1.5). Three candidate sites were identified: two in the S5-S6 linker and one in the S6 segment. Mutation of the proximal S5-S6 linker site failed to alter flecainide sensitivity. Mutation at the more distal site in Kv1.5 (V481L) modestly increased sensitivity, but the reciprocal Kv3.1 mutation (L401V) had no effect. S6 mutants caused marked changes: flecainide sensitivity decreased ~8-fold for Kv3.1 L422I (IC_{50}, 213 ± 9 μM) and increased ~7-fold for Kv1.5 I502L (IC_{50}, 35.6 ± 1.9 μM). Corresponding mutations reversed flecainide sensitivity of Kv1.4 and Kv4.2; L392I decreased Kv4.2 sensitivity by ~17-fold (IC_{50} of 37.4 ± 6.9 to 628 ± 36 μM); I547L increased Kv1.4 sensitivity by ~15-fold (IC_{50} of 706 ± 37 to 40.9 ± 7.3 μM). Our observations indicate that the flecainide sensitivity differences among these four voltage-gated K^+-channels are determined by whether an isoleucine or a leucine is present at a specific amino acid location.

Voltage-gated K^+-channels of the Shaker family play an important role in governing cardiac excitability (Roden and George 1997; Snyders, 1999). A variety of antiarrhythmic agents target Shaker-based channels (Tamargo et al., 2004; Varro et al., 2004), and such actions are believed to contribute to their actions in humans. The cardiac transient outward current (I_{to}) subunits Kv1.4 and Kv4.2 differ in their sensitivity to the antiarrhythmic drug flecainide; Kv4.2 is much more sensitive than Kv1.4. This difference has been used to probe the various contributions of Kv1.4 and Kv4.2 to native I_{to} in the rat (Yeola and Snyders, 1997). Kv1.5, the principal ionic current underlying human atrial ultrarapid delayed rectifier current (I_{Kur}) (Wang et al., 1993; Feng et al., 1997), is a potentially interesting atrium-selective ionic target for drug therapy of atrial fibrillation (Nattel et al., 1999). The dog counterpart, $I_{Kur.d}$, seems to have a contribution from Kv3.1 subunits (Yue et al., 1996, 2000b), although the importance of this contribution has recently been questioned (Fedida et al., 2003). In previous work, we found $I_{Kur.d}$ to be sensitive to flecainide (Yue et al., 2000a), unlike human I_{Kur}, which seems resistant (Wang et al., 1995). In preliminary studies, we observed corresponding differences in the flecainide sensitivity of Kv3.1 and Kv1.5 (Herrera et al., 2002), reminiscent of the differences typically observed between Kv4.2 and Kv1.4. The present study was designed to characterize flecainide block of Kv3.1 and Kv1.5 and then to determine whether there is a common molecular basis for differences in sensitivity to flecainide between Kv1.4 and Kv1.5 on one hand and Kv3.1 and Kv4.2 on the other.

We began by constructing several chimeras of the Kv3.1 and Kv1.5 wild-type channels to identify important domains

This work was supported by the Canadian Institutes of Health Research, the Quebec Heart and Stroke Foundation, and the Mathematics of Information Technology and Complex Systems (MITACS) Network.
Article, publication date, and citation information can be found at http://molpharm.aspetjournals.org.
doi:10.1124/mol.104.009506.

ABBREVIATIONS: WT, wild-type; d, dog; h, human; r, rat; CMV, cytomegalovirus; PCR, polymerase chain reaction; HERG, *human ether-a-go-go-related* gene.

of flecainide block in these channels. This was followed by site-directed mutagenesis of the identified domains to determine whether specific residues might modulate sensitivity of these channels to flecainide. The results of these studies pointed to a key role for the presence of leucine versus isoleucine at a specific amino acid location. Finally, a mathematical model was applied to assess the location and orientation of this amino acid in relation to key structures in the Kv3.1 channel molecule.

Materials and Methods

Molecular Biology. Wild-type (WT) dKv3.1 (GenBank accession no. AF153198), hKv1.5 (GenBank accession no. XM_006988; kindly provided by Dr. Barbara Wible, Case Western Reserve University Cleveland, OH) and rKv1.4 (GenBank accession no. NM_012971; kindly provided by Dr. Barbara Wible), were cloned into a pSP64 (Promega, Madison, WI) and rKv4.2 (GenBank accession no. S64320; kindly provided by Dr. Jeanne Nerbonne, Washington University, St. Louis, MO) into a pRC-CMV expression vector (Invitrogen, Carlsbad, CA) with identical restriction endonuclease sites flanking the clone in the polyclonal region for ligating the digest product into the target vector.

For chimera construction, we performed a series of polymerase chain reactions (PCRs) with Elongase enzyme mix (Invitrogen) and respective WTs as templates. For overlap extension of both products, we used a third PCR and the products of each of the previous reactions as the template. The synthetic oligonucleotide primers used for the first reactions contained the ends of the chimera and the restriction endonuclease sites for cloning into the expression vector (Table 1). The complementary primer contained part of one clone and an overlap overhang for the overlap extension PCR. The third PCR employed the end primers to create a continuous string of nucleotides of the desired sequence. The final products and target vectors were digested with appropriate restriction endonucleases (Table 1) and ligated with Quick T4 DNA ligase (New England Biolabs, Beverly, MA).

For site-directed mutagenesis, PCR was applied, with a synthetic oligonucleotide primer containing the desired nucleotide to create the point mutation upon translation. Two complementary primers containing desired mutation and PCR primers flanking unique restriction enzyme sites enclosed the region of interest. Two parallel PCR reactions, each with a flanking primer and a primer containing

TABLE 1
Primers used for chimera and point mutation construction

Clone	Primers	Annealing Temperatures		RES
		°C		
Kv3.1 I389D	1. CTGCCCCAACAAGATAGAGTTCAT	57	55	MscI
	2. CAGAAGCCATCGGGGATGTTCTTAAAGTGGG			BstEII
	3. GTCATGGTGACCACGGCCCACCAGAAGCCATCGGGGA			
Kv1.5 D469I	1. AGCGGGGTCATGGCCCCGCCCTCT	60	59	PmlI
	2. ACCAGAAGGCGATAGGGATGCTAG			BstEII
	3. CATGGTGACCACTGCCCACCAGAAGGCGATAGGGATGC			
Kv3.1 L401V	1. ATGACGACGGTGGGCTACGGAGAC	54	54	BstEII
	2. GCCCGTGGTCACCATGACGACGGTGGGCTAC			BamHI
	3. ATCGGATCCTCAAGTCACTCTCAC			
Kv1.5 V481L	1. AGTGGTCACCATGACCACTCTGGGCTACGGGGA	58		BstEII
	2. CATGATATCTCACAAATCTGTTTCCCGGCT			EcoRV
Kv3.1 L422I	1. GCACTGTGTGCGATAGCGGGCGTGCTG	53		BstAPI
	2. ATCGGATCCTCAAGTCACTCTCAC			BamHI
Kv1.5 I502L	1. TCCAGTGCCGTCTACTTCGCA	57	59	
	2. AGGACCCCGGCGAGGGCACACAGCGAG			BstEII
	3. GCTGTGTGCCCTCGCCGGGGTCCTCAC	57		EcoRV
	4. CATGATATCTCACAAATCTGTTTCCCGGCT			
Kv4.2 L392I	1. GGCCCTGGTGTTCTACTATGT	53	54	
	2. GACCAAGACTCCGCTAATTGAGCAGAT			BsmBI
	3. GGGTCTATCTGCTCAATTAGCGGAGTC	49		NotI
	4. ATAGTTTAGCGGCCGCGTCTTACAAAGCAGACAC			
Kv1.4 I547L	1. GCAGAGGCAGATGAACCTACC	53	54	
	2. TAAGACACCCGCAAGGGCACACAG			BsmI
	3. GGGTCCCTGTGTGCCCTTGCGGGTGTC	52		BamHI
	4. GATGGATCCTCAGACGTCAGTCTC			
Kv3.1/Kv1.5S6-Cterm	1. CAAGATAAGCTTATGGGCCAAGGGGACGAGAGCGAG	63	61	
	2. CCCGGCGATGGCACACAGCGAGCCCACGATCATGCCGGACCACGTCTGCGGGTA			HindIII
	3. GACATGTACCCGCAGACGTGGTCCGGCATGATCGTGGGCTCGCTGTGTGCCATC	63		SacI
	4. ACGAATGAGCTCTCACAAATCTGTTTCCCGGCTGGT			
Kv1.5/Kv3.1S6-Cterm	1. CAAGATAAGCTTATGGAGATCGCCCTGGTGCCCCTG	63	59	
	2. GCCCGCCAGCGCACACAGTGCTCCCACCAGCTTGCCCCCAACAGTGATGGGCCT			HindIII
	3. GACATGAGGCCCATCACTGTTGGGGGCAAGCTGGTGGGAGCACTGTGTGCGCTG	61		BamHI
	4. ACGAATGGATCCTCAAGTCACTCTCACAGCCTCTGT			
Kv3.1/Kv1.5Cterm	1. ATAGGGGCCCAGCCCAATGAC	59	49	54
	2. CACGATGACGGGCACAGGCAT			
	3. GTTGAAGTTGGACACGATGACGGG			BstEII
	4. TCCAACTTCAACTACTTCTACCACCGG	59	53	SacI
	5. ACGAATGAGCTCTCACAAATCTGTTTCCCGGCTGGT			
	6. CCCGTCATCGTGTCCAACTTCAACTACTTCTAC			
Kv1.5/Kv3.1Cterm	1. TCCAGTGCCGTCTACTTCGCA	48	55	
	2. GACGATGACGGGCACAGGCAG	57		
	3. CCCAAAATTGTTGACGATGACGGG			BstEII
	4. AACAATTTTGGGATGTATTACTCC	54		BamHI
	5. ACGAATGGATCCTCAAGTCACTCTCACAGCCTCTGT		54	
	6. CCCGTCATCGTCAACAATTTTGGGATGTATTACTCC			

RES, restriction endonuclease sites.

the desired mutation, generated two DNA fragments with overlapping ends. After gel purification, both fragments were annealed in a third PCR using the two restriction-site flanking primers, resulting in a fragment containing the desired mutation. The final PCR product was digested with the flanking restriction enzymes, gel-purified, and cloned into the PCRII vector with the use of TOPO TA (Invitrogen). All PCR-generated sequences were verified by double-stranded sequencing. After sequence confirmation, the mutant was released from PCRII at flanking restriction sites and ligated into pSP64 (or pRC-CMV) containing the coding region for the respective WT from which the segments enclosed by the restriction enzyme sites had been removed.

Oocyte Isolation. Frogs were anesthetized by immersion in tricaine methanesulfonate for approximately 25 min. Oocytes were excised and immersed in a 100-mm Petri dish containing Barth's solution (100 mM NaCl, 2.0 mM KCl, 1.8 mM $CaCl_2$, 1.0 mM $MgCl_2$, and 5.0 mM HEPES, pH adjusted to 7.4 with NaOH) at room temperature. Oocytes were physically separated, then immersed (~60 min) in 7 ml of calcium-free Barth's-collagenase solution containing 82.5 mM NaCl, 2.0 mM KCl, 1.0 mM $MgCl_2$, 5.0 mM HEPES, 0.0247 g of lyophilized collagenase type A (Invitrogen), and 0.0075 g of trypsin inhibitor. Oocytes were incubated in Barth's solution containing penicillin (1000 U/liter) (Invitrogen), streptomycin (100 mg/liter) (Invitrogen), kanamycin (100 mg/liter), and sodium pyruvate (275 mg/liter) (Sigma-Aldrich, St. Louis, MO) for 12 h at 15°C.

5′-Capped polyadenylated cRNA was prepared for each construct with the SP6 mMessage mMachine in vitro transcription kit (Ambion, Austin, TX) after cDNA linearization. *Xenopus laevis* oocytes were each injected with ~1 to 1.4 ng of cRNA using a microinjector and stored for at least 12 h in Barth's solution containing antibiotics and 5% horse serum at 15°C. Oocytes were placed in a recording/perfusion chamber and perfused at 0.5 ml/min with 5.0 mM KCl, 100 mM NaCl, 2.0 mM $MgCl_2$, 0.3 mM $CaCl_2$, 10 mM HEPES, pH adjusted to 7.4 with NaOH.

Data Acquisition and Analysis. Whole-cell currents were recorded at room temperature with 2-electrode voltage-clamp. Borosilicate-glass electrodes (o.d., 1.0 mm) filled with 3 M KCl (resistances 1–2 MΩ) were connected to a GeneClamp-500B amplifier (Axon Instruments, Union City, CA). Current-injecting electrode resistance averaged 1.5 MΩ. Voltage command pulses were generated with pClamp 6 software connected to a 12-bit Digidata 1200 analog-to-digital converter (Axon Instruments). A holding potential of −60 mV was used as in previous studies of native currents (Wang et al., 1995; Yue et al., 2000b). The effects of flecainide (Sigma-Aldrich) exposure were monitored with test pulses to +60 mV (in 10-mV steps). The interpulse interval was 10 s for all protocols, and pulse length is indicated in figure insets. Recordings were low-pass–filtered at 1 kHz. Data were analyzed with pClamp 6 (Axon Instruments) and are expressed as mean ± S.E.M. Group comparisons were performed with analysis of variance. If significant differences were indicated by analysis of variance, a *t* test with Bonferroni's correction was used to evaluate differences between individual mean values. A two-tailed $P < 0.05$ was taken to indicate statistical significance.

Homology Modeling of the Kv3.1 Pore. Two models of the Kv3.1 channel were generated using the KcsA (*Streptomyces lividans*) potassium channel (Protein Data Bank code 1J95) and the MthK (*Methanobacterium thermoautotrophicum*) potassium channel (Protein Data Bank code 1LNQ) structures as templates. The sequence alignment between the Kv3.1 pore-S6 region, MthK, and KcsA was performed with SAM-T02 (Hughey and Krogh, 1996). Automated homology modeling was carried out with Modeler V6.2 (Sali and Blundell, 1993) and involved the generation of 150 models of the Kv3.1 channel pore for each structural template. Model selection was based on the lowest objective function value (roughly related to the energy of the model) provided by Modeler (Sali and Blundell, 1993) and on the root-mean-square deviation between the atomic coordinates of the template relative to the model. Energy minimization was carried out on the four best models using Charmm (Brooks et al., 1983). The overall structural quality of the generated models was confirmed by PROCHECK (Laskowski et al., 1993). Structural features of flecainide were approximated using HyperChem 7.5 (Hypercube, Inc., Gainesville, FL) and the AMBER force field (Weiner et al., 1984).

Results

Effects of Flecainide on Kv3.1 and Kv1.5. The effects of flecainide on Kv3.1 WT and Kv1.5 WT were characterized by eliciting currents in response to pulses to potentials ranging from −50 to +60 mV in increments of 10 mV from a holding potential of −60 mV. Test pulses elicited rapidly activating outward currents with very slow inactivation in the absence of flecainide (Fig. 1). Reduced current increments were seen for Kv3.1 at potentials positive to +30 mV, compatible with inward rectification, as described previously for dKv3.1 (Yue et al., 1996, 2000b). Flecainide (50 μM) caused rapid decay of Kv3.1 currents upon depolarization, compatible with open-channel block, and potently decreased end-pulse current amplitude (Fig. 1A). Overall, 50 μM flecainide significantly inhibited dKv3.1 current at all voltages positive to 0 mV, with a mean 58.9 ± 3.9% reduction at +30 mV (Fig. 1B). In contrast, the same concentration of flecainide had little apparent effect on Kv1.5 currents (Fig. 1C), and mean Kv1.5 current amplitude was not significantly affected (Fig. 1D). These observations indicate important differences between Kv1.5 and Kv3.1 in their sensitivity to the drug.

Figure 2 shows the effects of the full range of drug concentrations on Kv3.1 and Kv1.5. Figure 2A illustrates the effects of increasing drug concentrations on current recorded upon stepping from −60 to +30 mV in single oocytes expressing each subunit. Flecainide appreciably decreased Kv3.1 current at 20 μM and produced near-total block of end-pulse current at 500 μM. In contrast, Kv1.5 was minimally affected by 50 μM flecainide, and 500 μM drug produced just over 50% inhibition. Figure 2B shows mean concentration-response data for flecainide inhibition of Kv3.1 and Kv1.5 at +30 mV. The flecainide IC_{50} values for Kv3.1 end-pulse current at + 30 mV averaged 28.3 ± 1.3 μM, with a Hill coefficient (n_H) of 0.91 ± 0.1 in 11 oocytes, an order of magnitude less than the corresponding value for Kv1.5 (237.1 ± 6.2 μM; n_H, 1.1 ± 0.2; $n = 8$ oocytes; $P < 0.001$). Figure 2C shows the percentage inhibition by two concentrations of flecainide on Kv3.1 and Kv1.5 at different test potentials. Inhibition showed shallow voltage-dependence for both subunits. At approximately equipotent flecainide concentrations (50 μM for Kv3.1 and 500 μM for Kv1.5), block as a function of voltage is not significantly different for the two subunits. Figure 2, D and E, show the activation curve for Kv3.1 and Kv1.5, respectively, based on an analysis of tail currents after 400-ms test pulses to various activation voltages, before and after exposure to approximately equipotent drug concentrations. The half-maximal activation voltage ($V_{1/2}$) of Kv3.1 was −1.7 ± 0.4 mV (slope factor, 8.2 ± 1.3 mV), and this was slightly shifted to −6.8 ± 1.5 mV ($P < 0.05$; slope factor, 7.4 ± 1.9 mV) after exposure to flecainide. For Kv1.5, the $V_{1/2}$ was −11.6 ± 1.8 mV (slope factor, 7.2 ± 1.8 mV) before and −16.9 ± 1.9 mV (slope factor, 7.4 ± 1.9 mV) after administration of 500 μM flecainide.

The rapid decay of current in the presence of flecainide

suggests open-channel blocking. Figure 3A, inset, shows the onset of Kv3.1 block as a function of time during the pulse at three concentrations of flecainide. Block was a discrete function of time, well fit by exponential relations as shown, and accelerated at higher drug concentrations. The regression lines in Fig. 3A are an analysis of blocking kinetics as a function of drug concentration. The blocking rate constant (K) was a linear function of concentration (C), consistent with a standard blocking model, $K = k_{off} + k_{on}[C]$ (where k_{off} and k_{on} are rate constants for drug-receptor association and dissociation). K is obtained from best-fit regression of the onset of block at each concentration to a single exponential function $B(t) = B_o + B_{td}(1 - \exp[-Kt])$, where $B(t)$ is block at time t, B_o is block upon pulse onset, and B_{td} = steady-state time-dependent block. The dissociation constant (K_d) is given by k_{off}/k_{on} and the exponential block-onset time constant τ_B at any concentration [C] is given by $1/(k_{on}[C] + k_{off})$, with the net rate constant K being $1/\tau_B$. When this relation was analyzed in each of eight experiments with Kv3.1, we obtained a mean k_{on} of $1.4 \pm 0.1\ \mu M^{-1}s^{-1}$ and k_{off} of $39.8 \pm 5.3\ s^{-1}$. The K_d estimated from k_{off}/k_{on} of the kinetic analysis averaged $28.8 \pm 3.6\ \mu M$, in good agreement with the directly measured IC_{50} (28.3 μM) as obtained in Fig. 2A. Figure 3B shows corresponding data for Kv1.5. The results are qualitatively similar, with lower blocking rates for a given concentration. For Kv1.5, k_{on} averaged $0.30 \pm 0.02\ \mu M^{-1}s^{-1}$ and k_{off} $60.0 \pm 5.5\ s^{-1}$ ($n = 8$ oocytes). K_d estimated from the kinetic analysis averaged $210.8 \pm 5.9\ \mu M$, once again in reasonable agreement with the directly measured IC_{50} (237 μM). Table 2 shows the calculated rate constants. The time-dependent block onset in Fig. 3, A and B, is compatible with open-channel block. This notion is further supported by observations of cross-over of control tail currents with those in the presence of blocking drug concentrations for Kv3.1 (Fig. 3C) and Kv1.5 (Fig. 3D). Upon repolarization in the absence of drug, rapid time-dependent transition of channels from the open to the closed state provides characteristic deactivating tail currents. In the presence of drug, deactivation of unblocked channels is similarly rapid. However, for many open-channel blockers, unblocking must occur in the open state; there is low affinity for the closed state, and drug-bound channels must unblock before closing. If a large fraction of channels have been blocked during depolarization and the unbinding rate k_{off} is fast enough, channels may unblock through the open state upon repolarization and carry significant current, thus slowing the apparent rate of deactivation. This process will be reflected in a slower time course of the tail current, resulting in tail current "cross-over" (Armstrong, 1971). The tail-current time course was fitted by monoexponential relations (as shown by the solid lines fitted to the experimental data points shown in Fig. 3, C and D), providing the mean data shown in Fig. 3E. These results show that the rate of current decay upon repolarization was prolonged significantly in the presence of drug. Kv3.1 tail-current time constants increased from 54.8 ± 2.7 ms (control) to 218.2 ± 9.6 ms in presence of flecainide 50 μM ($P = 0.0017$, $n = 8$ oocytes). Corresponding values for Kv1.5 before and after 100 μM flecainide were 115.6 ± 3.0 ms and 247.4 ± 7.2 ms, respectively ($P = 0.0173$, $n = 8$ oocytes).

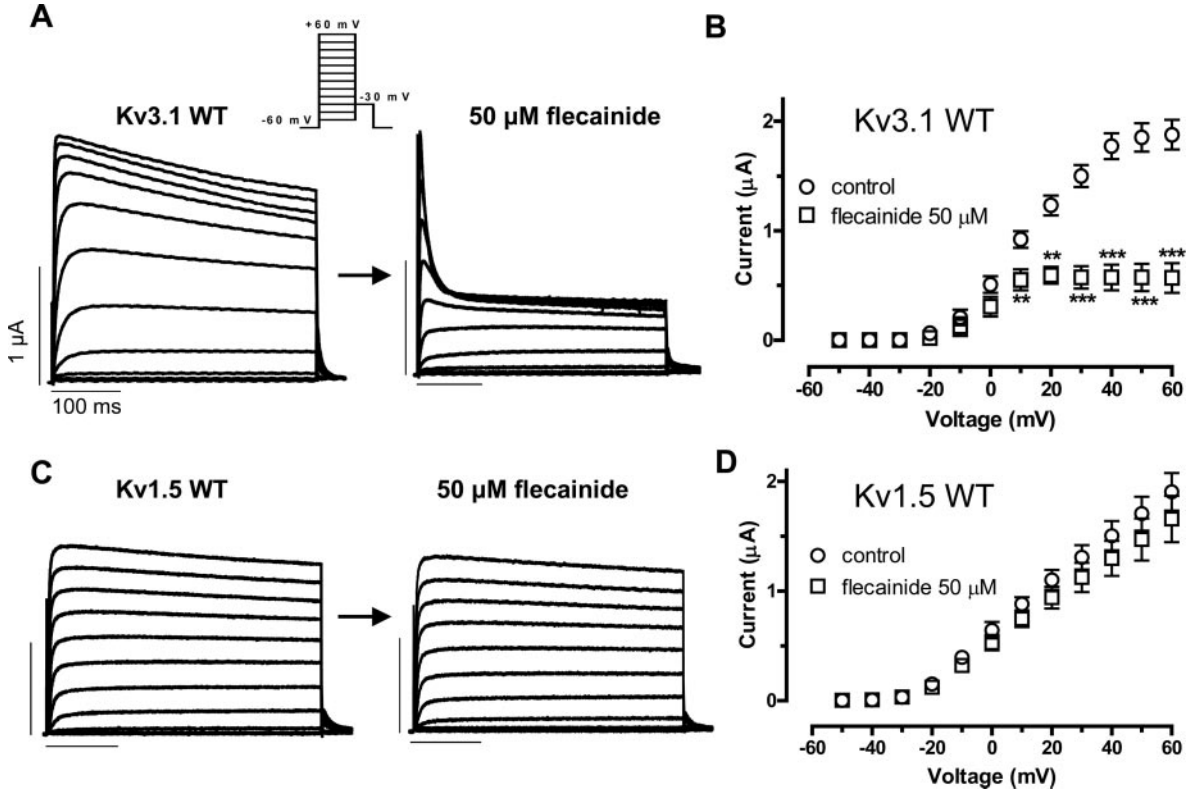

Fig. 1. Flecainide inhibition of Kv3.1 and Kv1.5 currents expressed in *X. laevis* ($n = 8$ per observation). Kv3.1 (A) and Kv1.5 (C) currents induced by depolarization to potentials ranging from −50 mV to +60 mV from a holding potential of −60 mV in the absence and presence of 50 μM flecainide. Inset, voltage clamp protocol used to elicit currents. Vertical scale bars, 1 μA; horizontal scale bars, 100 ms. Current-voltage relationships for Kv3.1 (B) and Kv1.5 (D) currents in the absence (○) and presence of 50 μM flecainide (□) (**, $P < 0.01$; ***, $P < 0.001$ versus control).

Response of Kv3.1/Kv1.5 Chimeras to Flecainide. As an initial approach to analyzing the molecular determinants of the differential flecainide sensitivity of Kv3.1 and Kv1.5, we constructed chimeras between the two subunits. Two sets of reciprocal chimeras were constructed. Because we had already observed block of the wild-type channels in their open configuration, we decided to concentrate on the pore to C-terminal region (see Fig. 3, C–E). One set of chimeras involved the C-terminal distal to position Asn-436 in Kv3.1 and Asn-518 in Kv1.5. Figure 4A, top, shows typical recordings before and after 50 μM flecainide in WT Kv3.1 and Kv1.5, whereas Fig. 4A, middle, shows corresponding recordings from Kv3.1 subunits with their C-terminal replaced by those of Kv1.5 and Kv1.5 subunits with Kv3.1 C-terminal substitution. There was clearly no major change in sensitivity. We therefore interchanged longer segments of each subunit, involving the C terminus distal to Met-414 in the Kv3.1 S6 segment and Lys-494 in the Kv1.5 S6. Figure 4A, bottom, shows that flecainide sensitivity was somewhat decreased for Kv3.1 subunits containing the S6+C-terminal component of Kv1.5 and that sensitivity was increased for the corresponding Kv1.5 chimera. Figure 4B compares mean ± S.E.M. concentration-response data for the S6+C-terminal chimeras with those of WT at +30 mV. Results for the chimeras clearly lie in a position different from those of the WT and close to each other. Mean IC_{50} values at +30 mV based on values calculated for each oocyte studied for WT and both sets of chimeric constructs are shown in Fig. 4C. Whereas values for the C-terminal chimeras are indistinguishable from WT, values for the S6+C-terminal chimeras are significantly different from their respective WTs and not different from each other. These results suggest that molecular motifs in S6 play a role in determining the flecainide affinity differences between Kv3.1 and Kv1.5. We next proceeded to address the potential role of specific amino acid residues in these drug affinity differences.

Effects of Mutating Candidate Amino Acids in Kv3.1 and Kv1.5 on Flecainide Sensitivity. The results described above suggest that flecainide produces open-channel block of both Kv3.1 and Kv1.5, with marked differences in affinity. We noted that similar differences in flecainide affinity had previously been reported for Kv1.4 (Yamagishi et al., 1995), which, like its Kv1 subfamily co-member Kv1.5, is flecainide-insensitive, and Kv4.2 (Caballero et al., 2003), which is typically flecainide-sensitive. In addition, we noted that many of the amino acids that determine drug block of

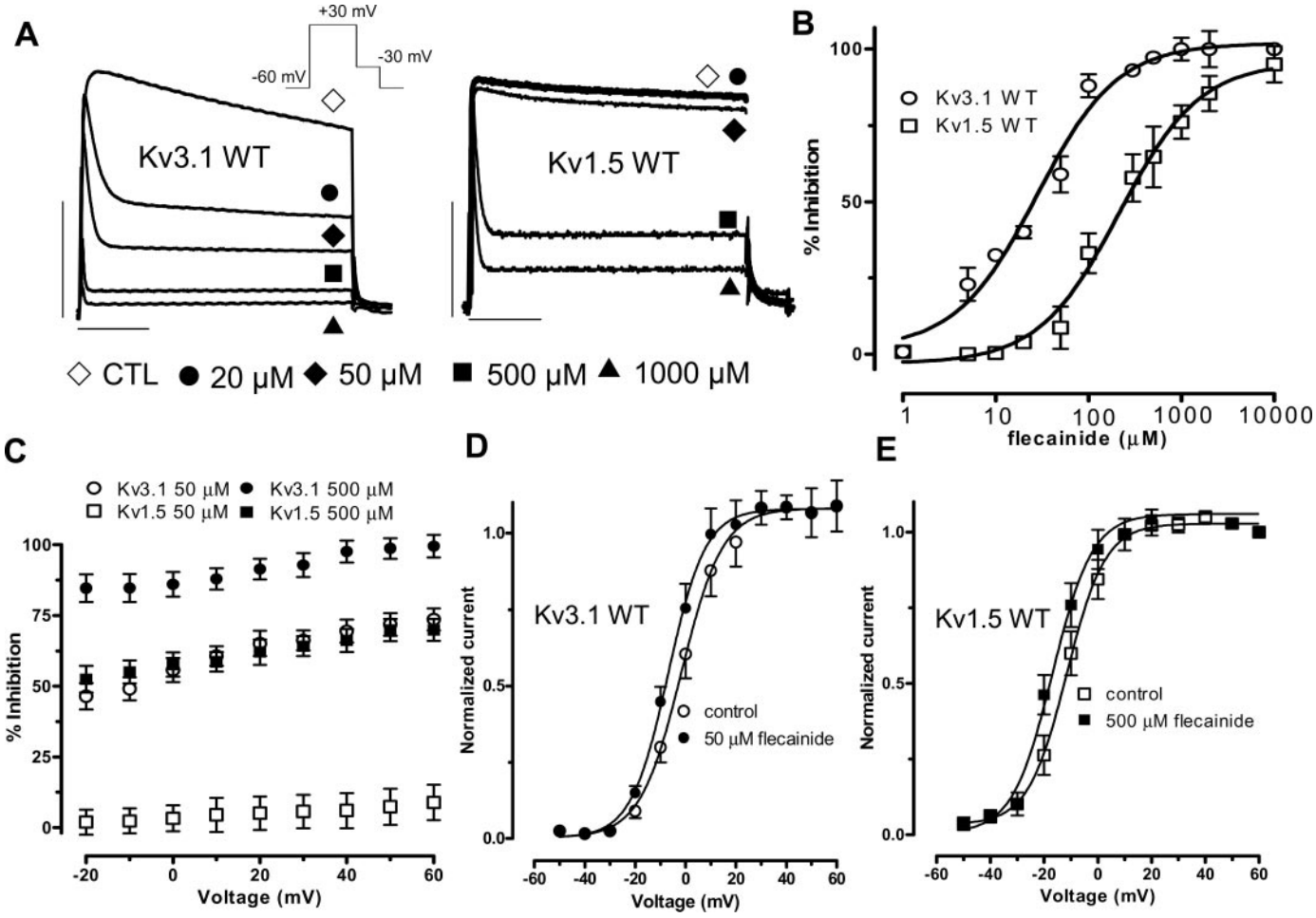

Fig. 2. A, effects of four concentrations of flecainide on currents recorded in representative oocytes expressing Kv3.1 and Kv1.5 (protocol in inset). Note that all recordings before and after drug were in the same oocyte. Vertical scale bars, 1 μA; and horizontal scale bars, 100 ms. B, concentration-response curves for Kv3.1 and Kv1.5 (mean ± S.E.M.) for effects of flecainide upon steps to +30 mV (n = 8 per observation). C, percentage reduction (mean ± S.E.M.) in Kv3.1 and Kv1.5 as a function of test potential at 50 and 500 μM flecainide. D and E, activation voltage-dependence of Kv3.1 and Kv1.5 currents under control conditions and in the presence of 50 and 500 μM flecainide, respectively, as determined based on the tail current at −30 mV after steps to each of the voltages indicated normalized to the tail current after a step to +60 mV (n = 8 per observation).

voltage-dependent K^+-channels are situated in the S5-S6 linker region or in S6 (Yeola et al., 1996; Franqueza et al., 1997; Zhang et al., 1998; Caballero et al., 2002; Decher et al., 2004). We therefore aligned and compared these portions of the sequences of rKv1.4, hKv1.5, dKv3.1, and rKv4.2 with one another. As shown in Fig. 5, there was a large degree of homology among these subunits. At three positions (shown by boxes and symbols corresponding to their respective position in the channel protein), amino acid residues corresponded for Kv1.4 and Kv1.5, on one hand, and for Kv3.1 and Kv4.2, on the other, but differed between the sensitive and insensitive subunits.

We therefore considered these three amino acid residues to be candidates to play a role in the difference in flecainide sensitivity between the sensitive subunits Kv3.1 and Kv4.2 and the insensitive subunits Kv1.4 and Kv1.5. We first used site-directed mutagenesis to alter each of these amino acids in Kv3.1 to those in Kv1.5 and to alter the amino acids in Kv1.5 to those in Kv3.1. Figure 6A illustrates the effects of several flecainide concentrations on current at +30 mV in oocytes expressing WT subunits and each of the point mutations. The response of Kv3.1 subunits with the I389D mutation was similar to that of the WT subunits shown immediately above. Likewise, Kv1.5 with the reciprocal D469I mutation responded like Kv1.5 WT. The response of L401V Kv3.1 also resembled that of Kv3.1 WT, but the reciprocal V481L Kv1.5 seemed somewhat more sensitive to flecainide than Kv1.5 WT. The mutations shown in Fig. 6A, bottom, had quite striking effects. The L422I mutation strongly decreased the sensitivity of Kv3.1, whereas I502L strongly increased that of Kv1.5.

Figure 6B shows the mean IC_{50} values for each of the constructs studied at +30 mV. The isoleucine/aspartic acid mutations did not alter the IC_{50} of either Kv3.1 or Kv1.5. Whereas Kv3.1 L401V had an IC_{50} indistinguishable from that of Kv3.1 WT, Kv1.5 V481L had a significantly lower IC_{50} than that of Kv1.5 WT. The most striking changes occurred with the isoleucine/leucine mutations in the S6 segment. The IC_{50} of Kv3.1 L422I was dramatically increased from that of Kv3.1 WT and approached the value of Kv1.5 WT. Likewise, the IC_{50} of Kv1.5 I502L was substantially decreased and approximated that of Kv3.1 WT. The full concentration-response relations for flecainide inhibition of the reciprocal isoleucine/leucine mutants and their respective WTs are shown in Fig. 6C. They indicate that the S6 isoleucine/leucine mutants transformed the flecainide-sensitivity phenotype of each subunit to resemble that of its opposite WT counterpart. Table 2 shows the rate constants for leucine/isoleucine mutants compared with WT and indicates that, like the WT channels, the main differences among the mutants was in the k_{on}, suggesting that the differences in drug

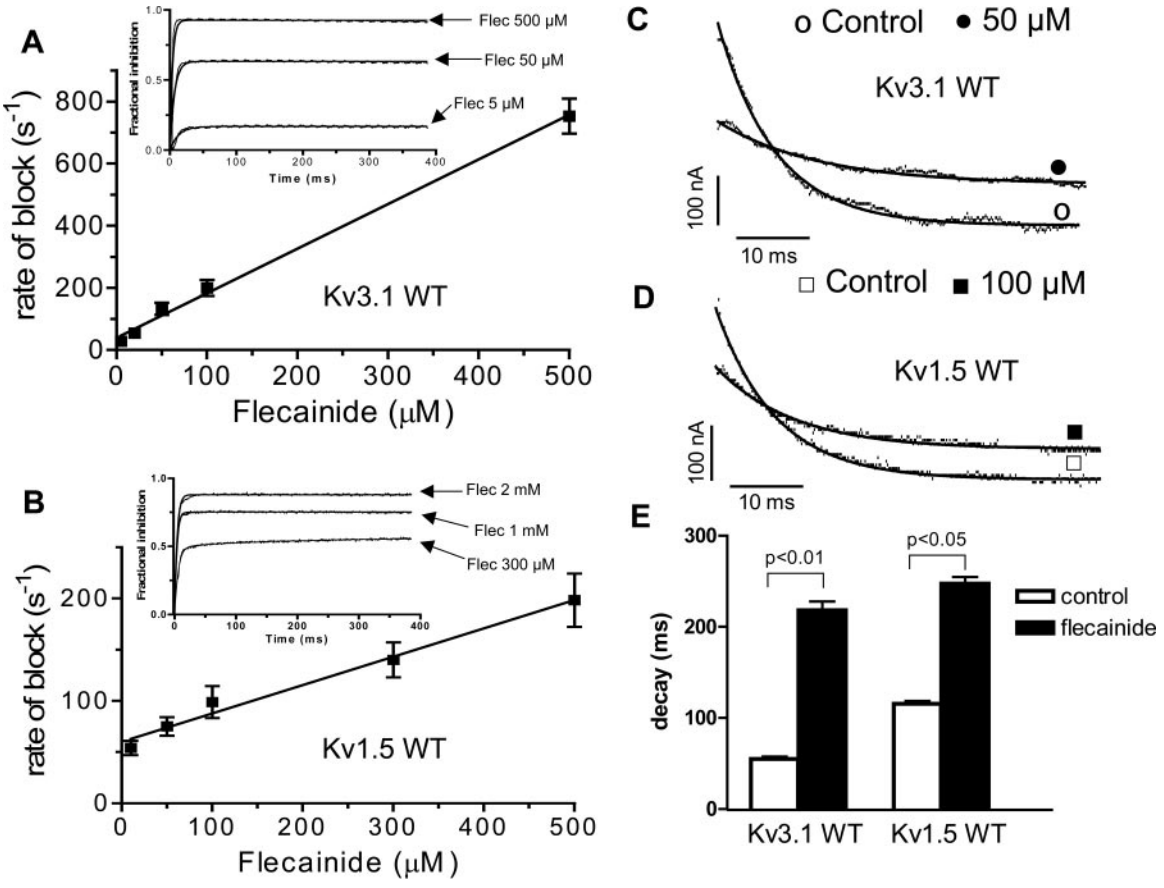

Fig. 3. Time-dependent flecainide effects. A and B, mean ± S.E.M. blocking rate constants (determined as illustrated in insets) were a linear function of flecainide concentration (n = 8 oocytes/data point). Inset, fractional inhibition of Kv3.1 (A) and Kv1.5 (B) current produced by the flecainide concentration indicated relative to control (given by $[(I_{Ctl} - I_{Flec})/I_{Ctl}]$) are shown as a function of time during voltage steps to +30 mV. Original data are shown, as well as best-fit exponentials to determine the rate constants for block onset. C and D, tail currents were elicited upon repolarization to −30 mV after pulses to +60 mV from a holding potential of −60 mV. Kv3.1 (C) and Kv1.5 (D) deactivation currents (tail currents) in the absence and presence of the indicated flecainide concentration. E, summary data (mean ± S.E.M.) of time course of deactivation in the absence and presence of flecainide concentrations indicated in C and D (results were obtained in eight oocytes per construct).

sensitivity were due to differences in drug access to the channel rather than stability of the drug-receptor complex.

Biophysical Effects of the S6 Isoleucine/Leucine Mutations in Kv3.1 and Kv1.5. To evaluate changes in biophysical properties as potential mechanisms of altered flecainide sensitivity of the S6 Kv3.1 and Kv1.5 mutants, we assessed the kinetics, activation, voltage-dependence and reversal potentials of the currents carried by the various constructs. As shown in Table 3, despite the substantial changes in flecainide-sensitivity caused by the mutations, they did not affect the primary biophysical properties of the channels.

Effects of Corresponding Mutations in Kv1.4 and Kv4.2. The striking changes in Kv3.1 and Kv1.5 flecainide sensitivity caused by the S6 isoleucine/leucine mutations suggest a crucial role in determining the flecainide sensitivity differences between these subunits. To determine the role of the corresponding residues in Kv1.4 and Kv4.2, we made the equivalent point mutations in these subunits. The results are illustrated in Fig. 7. Figure 7A, left, shows currents recorded upon voltage steps from −80 mV in Kv4.2 WT, Kv4.2 with the S6 L492I mutation, Kv1.4 WT, and Kv1.4 I547L. Figure 7A, right, shows currents recorded from the same oocytes after exposure to 50 μM flecainide. Kv4.2 WT was clearly flecainide-sensitive, and Kv1.4 WT was flecainide-insensitive. L392I abolished the response to 50 μM flecainide in Kv4.2 without obviously affecting current kinetics. On the other hand, the reciprocal mutation in Kv1.4 substantially increased flecainide sensitivity. Figure 7B shows the full concentration-response relations for the WT subunits and the isoleucine/leucine mutants at +30 mV. The mutations clearly reversed the flecainide-sensitivity differences, with curves for each point-mutated subunit superimposed on the curve of the opposite WT subunit. Overall, Kv4.2 WT exhibited marked sensitivity to flecainide with an IC_{50} of 37.4 ± 6.9 μM, compared with Kv1.4 WT, which had an IC_{50} of 706.3 ± 37.2 μM ($P < 0.001$ versus Kv4.2). The Kv1.4 I547L mutant IC_{50} was decreased to 40.9 ± 7.3 μM ($P < 0.001$ versus Kv1.4 WT), whereas the flecainide IC_{50} of the Kv4.2 L392I mutant was 628.3 ± 35.5 μM ($P < 0.001$ versus Kv4.2 WT).

TABLE 2
Rate constants for wild-type and mutant channels

Channel	k_{on}	k_{off}	K_d
	$\mu M^{-1}s^{-1}$	s^{-1}	μM
Kv3.1 WT	1.4 ± 0.1	39.8 ± 5.3	28.8 ± 3.6
Kv3.1 L422I	0.37 ± 0.05	73.2 ± 4.5	202.7 ± 11.7
Kv1.5 WT	0.30 ± 0.02	60.0 ± 5.5	210.8 ± 5.9
Kv1.5 I502L	1.1 ± 0.3	36.7 ± 1.6	35.4 ± 1.9

Discussion

In this study, we have evaluated the basis for pharmacological sensitivity differences among four voltage-dependent

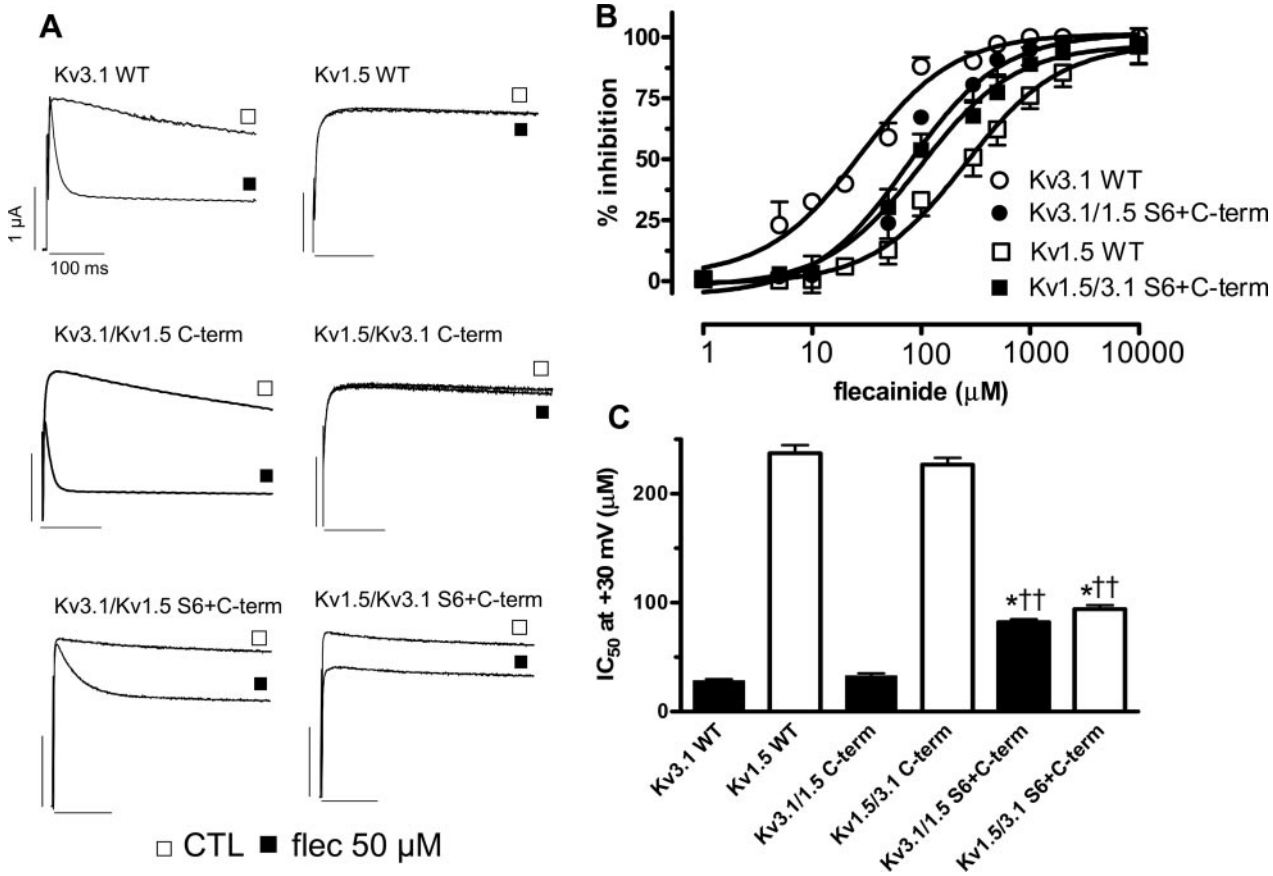

Fig. 4. Effects of flecainide on currents carried by WT and chimeric subunits. A, current recordings in absence and presence of 50 μM flecainide. B, concentration-response curves for Kv3.1 WT, Kv3.1 with the Kv1.5 S6 and C terminus (Kv3.1/Kv1.5 S6+C-term), Kv1.5 WT and Kv1.5 with the Kv3.1 S6 and C terminus (Kv1.5/Kv3.1 S6+C-term). C, IC_{50} values for flecainide effects on currents upon application of a pulse to +30 mV. (*, $P < 0.05$ versus Kv3.1 WT; ††, $P < 0.01$ versus Kv1.5 WT, $n = 6–8$). Vertical calibrations, 1 μA; horizontal calibrations, 100 ms. Kv3.1/1.5C-term, chimera formed by substituting Kv1.5 C terminus into Kv3.1; Kv1.5/3; 1C-term, chimera formed by substituting Kv3.1 C terminus into Kv1.5.

K^+-channel subunit channels. We find that a single, relatively conservative amino acid difference in S6 accounts for the variations in flecainide sensitivity.

Comparison with Previous Studies of Molecular Determinants of Cardiac Ion-Channel Block. Replacing a leucine with an isoleucine in corresponding positions of the S6 transmembrane domain conferred to the flecainide-sensitive channels Kv3.1 and Kv4.2 a flecainide affinity similar to that of the insensitive subunits Kv1.4 and Kv1.5. Mutating the equivalent isoleucine in Kv1.4 and Kv1.5 to a leucine conferred strongly increased sensitivity similar to that of Kv3.1 and Kv4.2. These subunits possess highly conserved S5, pore, and S6 segments.

Several previous studies have examined molecular motifs in these subunits that determine antiarrhythmic drug binding (Yeola et al., 1996; Franqueza et al., 1997; Caballero et al., 2002; Decher et al., 2004). Yeola et al. (1996) were the first to examine the determinants of quinidine binding in Kv1.5. They noted that residues in the S6 segment, specifically Thr-507 and Val-514, are significant determinants of

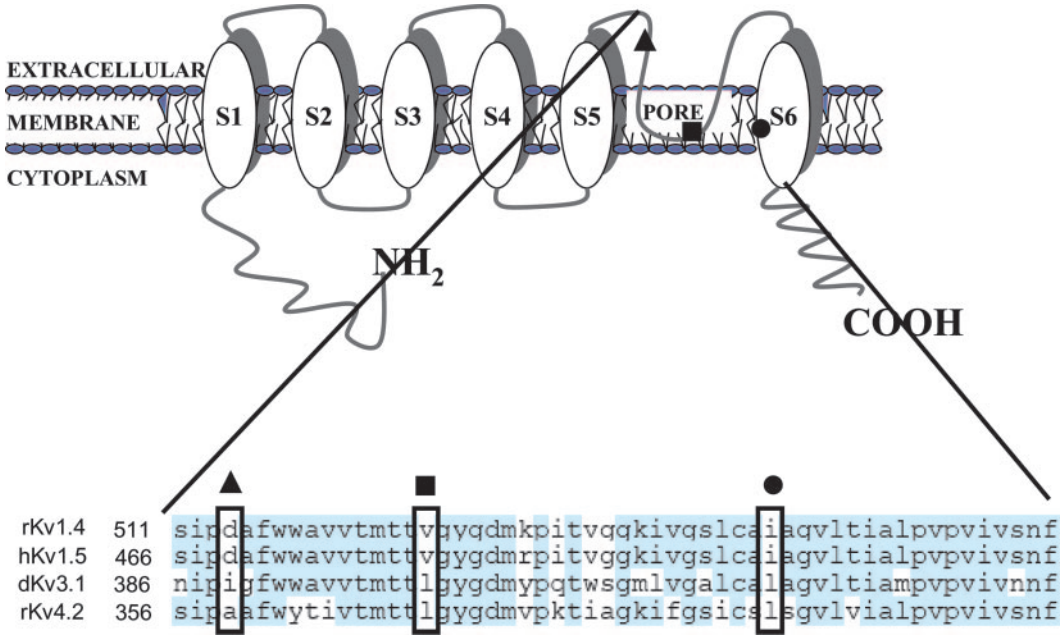

Fig. 5. Amino acid sequence comparison of the region between the beginning of the S5-S6 linker and S6 in dKv3.1, hKv1.5, rKv4.2, and rKv1.4. Residues selected for mutation analysis are boxed.

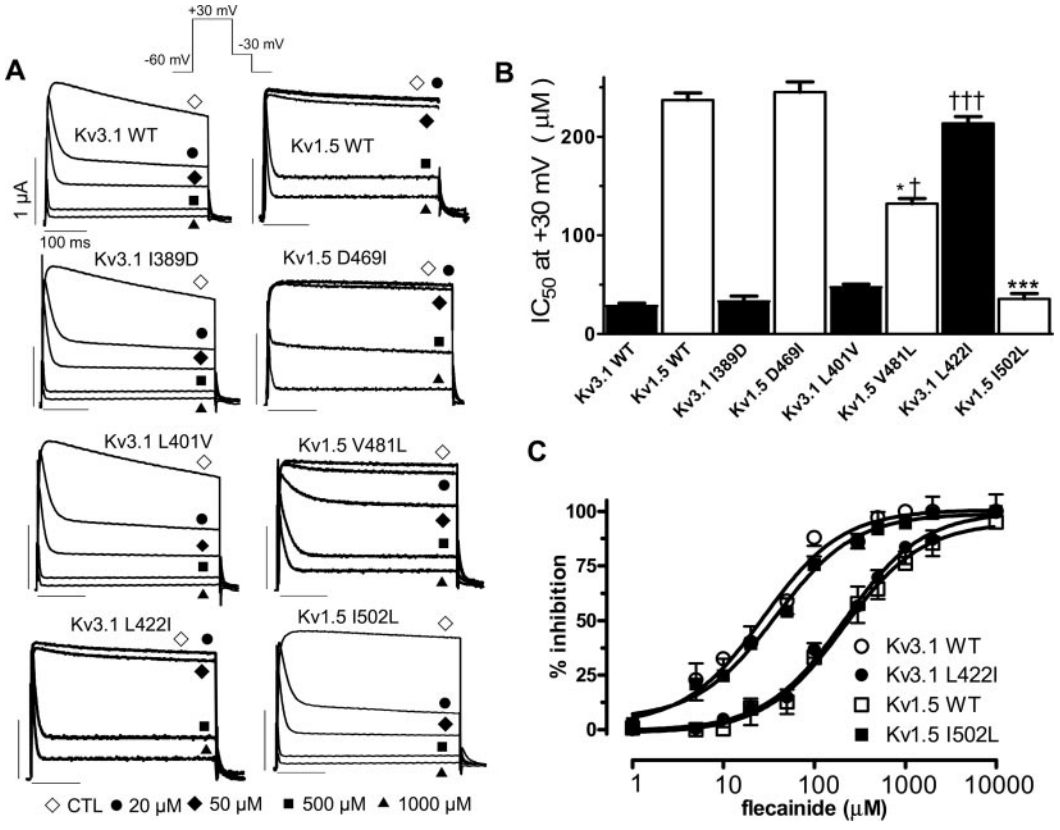

Fig. 6. A, effects of four concentrations of flecainide on currents recorded in representative oocytes expressing WT and various mutant constructs of Kv3.1 (left) and Kv1.5 (right) (voltage protocol in inset). Vertical calibrations, 1 μA; horizontal calibrations, 100 ms. B, mean ± S.E.M. IC_{50} values for WT and mutant constructs (*, $P < 0.05$; ***, $P < 0.001$ versus Kv1.5WT; †, $P < 0.05$; †††, $P < 0.001$ versus Kv3.1 WT, $n = 6–8$ per data point). C, concentration-response curves for WT and isoleucine/leucine mutants mean ± S.E.M. for effects of flecainide upon steps to + 30 mV ($n = 6–8$ per data point).

quinidine block. Franqueza et al. (1997) showed that mutations at Thr-507, Leu-510, and Val-514 abolish stereoselectivity of bupivacaine block of Kv1.5. Caballero et al. (2002) examined the determinants of benzocaine block and low-concentration agonist activity on Kv1.5, and found that mutations of Thr-479, Thr-507, Leu-510, and Val-514 abolish agonist actions but increase blocking effects. In a recent study, Decher et al. (2004) used alanine-scanning mutagenesis to examine the role of 23 amino acids in the K^+-signature sequence and S6 of Kv1.5 in sensitivity to the anthranilic acid derivative S0100176. Mutations at Thr-479, Thr-480, Val-505, Ile-508, and Val-512 reduced drug sensitivity. An alanine mutation at Ile-502, the critical site in the present study, slightly but significantly decreased sensitivity to S0100176. The authors concluded that specific S6 and pore helix residues facing the inner cavity form a binding pocket for S0100176. There is also evidence for a role of S6 residues in determining drug block of Kv1.4 channels. Substitutions at T529 alter sensitivity to quinidine and 4-aminopyridine, with a phenylalanine substitution in particular strongly reducing the affinity for quinidine (Zhang et al., 1998). Phenylalanine substitutions in the leucine heptad repeat region of the S4-S5 linker region stabilize the closed state of Kv1.4 and increase 4-aminopyridine sensitivity (Judge et al., 2002).

There is evidence for an important role of S6 residues in governing drug block of other cardiac voltage-gated potassium channels. Mutations at Ser-620 and Ser-631 impair C-type inactivation of the rapid delayed-rectifier channel encoded by the *human ether-a-go-go-related* gene (HERG) and attenuate verapamil block (Zhang et al., 1999). Changes in HERG inactivation caused by S6 mutations can be dissociated from alterations in blocking drug affinity, suggesting a primary role for modulation of drug affinity rather than state-dependent block (Lees-Miller et al., 2000). An elegant series of studies from Dr. Sanguinetti's laboratory have revealed the structural basis for HERG block, with cation-π interactions involving critical S6 residues and tertiary nitrogens playing a central role (Mitcheson et al., 2000; Fernandez et al., 2004). Likewise, S6 domain residues are crucial determinants of drug block of the slow delayed-rectifier channel KvLQT1 (Seebohm et

TABLE 3
Biophysical properties of wild-type and mutant clones

Clone	$V_{1/2}$	k	τ_{-10mV}	τ_{+30mV}	V_{rev}
	mV		*ms*		*mV*
Kv3.1 WT	−1.7 ± 0.4	8.2 ± 1.1	19.4 ± 1.5	3.9 ± 0.5	−78 ± 3.2
Kv3.1 L422I	−2.1 ± 0.5	8.0 ± 1.5	18.7 ± 1.9	3.5 ± 0.9	−76 ± 4.8
Kv1.5 WT	−11.6 ± 1.8	7.2 ± 1.2	9.8 ± 1.1	2.7 ± 0.3	−73 ± 3.4
Kv1.5 I502L	−10.3 ± 1.7	7.0 ± 1.4	9.6 ± 1.6	2.5 ± 0.6	−74 ± 4.6

$V_{1/2}$, 50% activation voltage; k, slope factor of activation curve; τ_{-10mV}, τ_{+30mV}, activation time constants at −10 and +30 mV, respectively; V_{rev}, reversal potential based on reversal of tail currents following a 25-ms activating pulse to +30 mV.

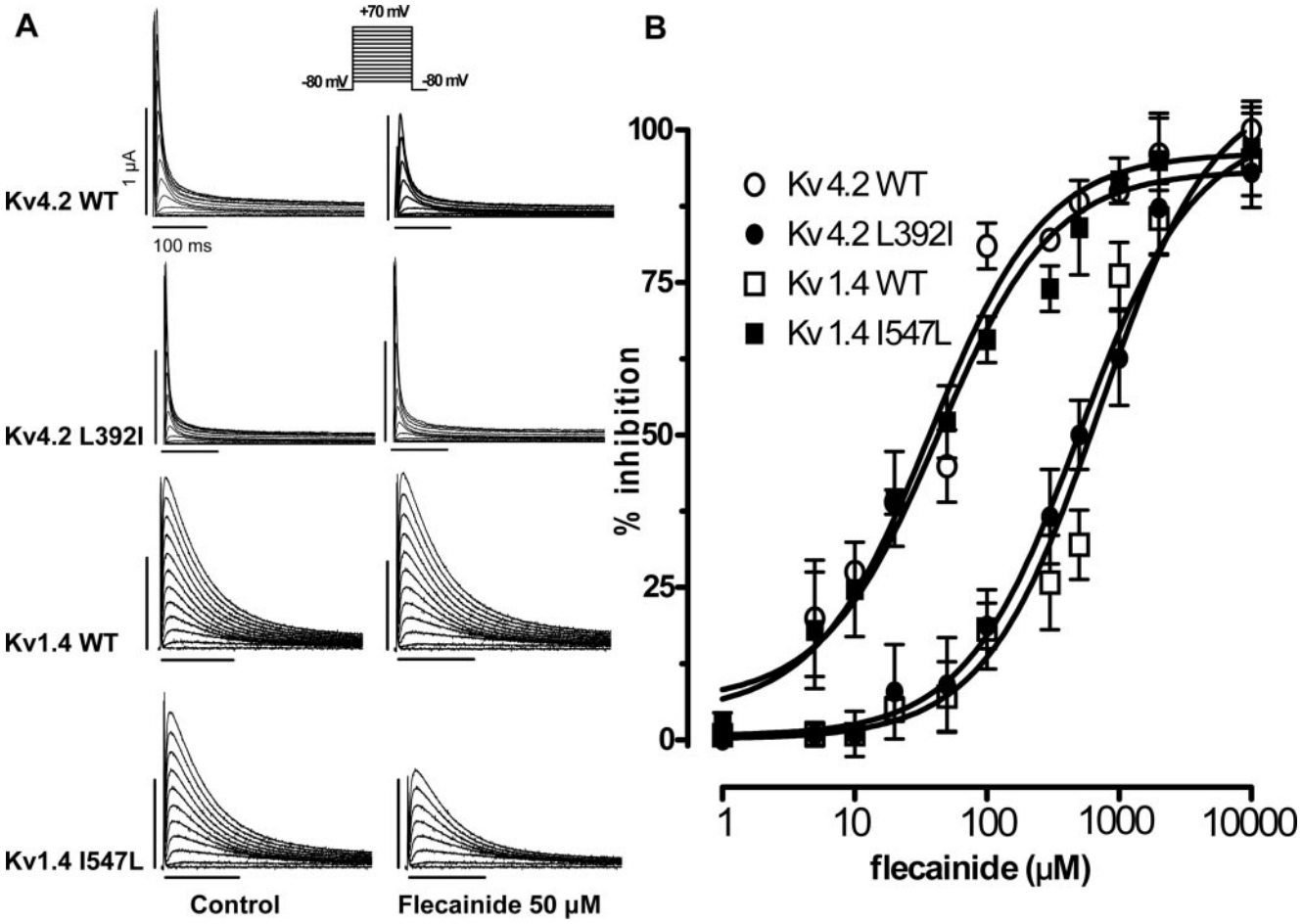

Fig. 7. Effects of flecainide on I_{to}-forming subunits. A, current recordings of Kv4.2 WT, Kv4.2 L392I, Kv1.4 WT, and Kv1.4 I547L in the absence (left) and presence (right) of 50 μM flecainide (recordings before and after drug were always obtained in the same oocyte). B, concentration-response curves for flecainide inhibition of currents elicited by depolarization to +30 mV. Vertical calibrations, 1 μA; horizontal calibrations, 100 ms.

al., 2003), voltage-gated Na^+-channels (Ragsdale et al., 1996; Sunami et al., 1997), and L-type Ca^{2+}-channels (Hockerman et al., 1997).

Model of Kv3.1 Channel Pore. We used molecular modeling to evaluate the position of the critical leucine/isoleucine amino acid residue in relation to key structural components of Kv3.1. The results of structural modeling (according to the approach described under *Materials and Methods*) are shown in Fig. 8. The overall structure of the S5-pore-S6 region of Kv3.1 is illustrated in a ribbon representation, with the surface of the Leu-422 and Val-425 residues colored in yellow and red, respectively. The Val-425 residue is seen as projecting inside part of the channel central cavity (Jiang et al., 2002). This residue has been shown to participate in the binding of a large number of inhibitory agents to several K^+ channels, including the voltage-gated Shaker (Liu et al., 1997) and the KCa3.1 (Wulff et al., 2001) channels. Because the dimensions of the channel inner cavity (10 Å) correspond to the computed length of a flecainide molecule, it is quite conceivable that flecainide interacts directly with the hydrophobic residues of the channel cavity, particularly Val-425. In contrast, the van der Waals' surface of the key Leu-422 residue appears to be projecting directly behind Val-425.

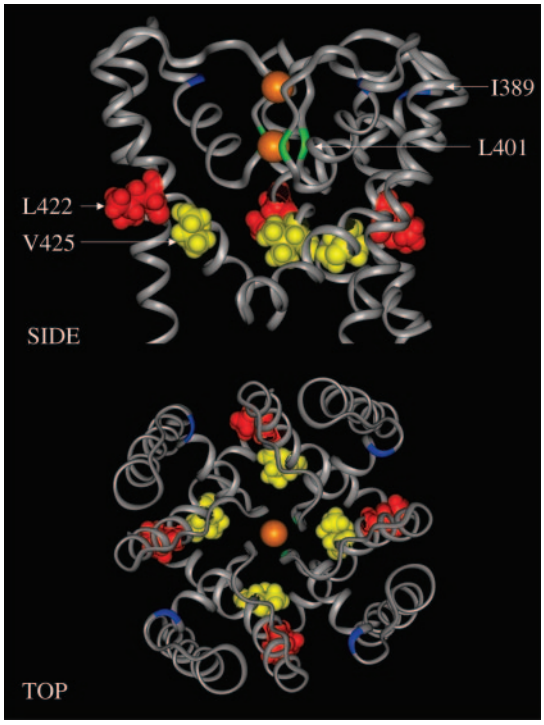

Fig. 8. Homology model of the Kv3.1 pore. Structural model of the Kv3.1 pore region obtained by homology modeling using the MthK crystal structure as template (Protein Data Bank code 1LNQ). Top and side views of the predicted Kv3.1 channel S5-Pore-S6 region shown in a ribbon representation. The channel selectivity filter is illustrated containing two K^+ ions (orange). The Leu-422 (red) and the cavity-lining residue Val-425 (yellow) are represented as van der Waals surfaces. Only three of the four monomers have been included in the side view representation of the channel for clarity. This model predicts that the Leu-422 residue is positioned behind Val-425. As a result, Leu-422 is not expected to face the channel central cavity and thus to interact directly with flecainide. The position of the hydrophilic Leu-401 and Ile-389 residues has been marked in green and blue, respectively. The Ile-389 residue is predicted to be located in the N-terminal end of the channel pore helix (blue), whereas the Leu-401 residue is seen as part of the selectivity filter. Mutation of these residues is not expected to affect the structure of the channel central cavity, where binding of flecainide is most likely to take place.

Hence, our structural analysis does not support a direct interaction between flecainide and the residue at position 422; therefore, it is probably not part of the binding site per se. It is possible, however, that the Leu-to-Ile mutation at position 422 induces a repositioning of the V425 residue, thereby modifying the interaction between flecainide and residues such as V425 in the channel cavity. On the other hand, as seen in the model in Fig. 8, Leu-422 is located directly above the highly conserved Gly-424 residue, which is generally considered to act as a gating hinge. This residue bends the inner helix by approximately 30° in the crystal structure of MthK and is believed to provide part of the S6 segment flexibility required for Kv channel opening. It is thus possible that the L422I mutation alters the flexibility of the Gly-424 region, thus modulating the rate at which flecainide has access to the channel inner cavity.

Figure 8 also includes the position of the hydrophilic Leu-401 (green) and Ile-389 (blue) residues, mutation of which failed to alter flecainide sensitivity of Kv3.1. The Ile-389 residue is predicted to be located in the N-terminal end of the channel pore helix (blue), whereas the Leu-401 residue is seen as part of the selectivity filter (Doyle et al., 1998). Because Ile-389 is more exposed to the external medium than to the internal medium, mutating this residue is not expected to affect the structure of the channel central cavity. However, according to the proposed model, the leucine at position 401 could indirectly modify the position of the cavity-lining T400 residue and thus affect flecainide binding. In fact, residues at positions equivalent to Thr-400 have been implicated in drug binding (e.g., Wulff et al., 2001). However, mutation of Leu-401 is not likely to result in a significant change in the Thr-400 orientation because of the high rigidity of the filter region.

The predicted positions of the Ile-389, Leu-401, Leu-422, and Val-425 residues depend on the validity of our homology-based models. In this regard, it should be pointed out that the structural features of the Leu-401, Leu-422, and Val-425 residues are conserved whether Kv3.1 is modeled with MthK (Fig. 8) or with the closed KcsA channel structure as template (data not shown). The structure of the S6 segment above the gating-hinge glycine residue thus seems to change minimally between the closed and the open conformation of K^+-channels, despite important structural changes in the C-terminal region of S6. However, in the absence of a crystal structure for mammalian voltage-gated K^+ channels, we cannot rule out the possibility that the orientation of the Leu-422 and Val-425 residues differs from that predicted by the bacterial MthK and/or KcsA structures. Further studies to evaluate the potential structural basis for the role of the isoleucine/leucine moiety in determining flecainide sensitivity, as well as the importance of other residues in that region, would be of interest.

Potential Importance of Our Findings. The difference in flecainide sensitivity between Kv1.4 and Kv4.2 is well recognized; flecainide has consequently been used as a tool to explore the potential molecular basis of native I_{to} (Yeola and Snyders, 1997; Han et al., 2000a). Flecainide sensitivity differences have also been noted between canine I_{Kur} with properties of Kv3.1 (Yue et al., 2000a) and native human Kv1.5-like I_{Kur} currents (Wang et al., 1995). The present study demonstrates a common molecular basis for these sensitivity differences: the presence of a leucine rather than an isoleu-

cine at a key S6 amino acid position in the flecainide-sensitive subunits.

Atrial fibrillation is the most common clinical arrhythmia and its treatment remains suboptimal (Nattel et al., 2002). Because of its atrial-selective localization, Kv1.5-based human I_{Kur} has been suggested to be a potentially interesting target for new antiarrhythmic drug development (Wang et al., 1993). The present study was designed to shed light on the molecular determinant of reported differences seen between sensitive and insensitive subunits. The identification of a key amino acid determinant is an important step in this direction. A better understanding of the molecular determinants of the drug sensitivity of Kv1.5 and related channels may help in the rational design of new antiarrhythmic compounds.

Potential Limitations. The objective of this study was to determine the molecular basis for the differences in flecainide sensitivity among four subunits involved in forming native K^+-channels for which discrepancies in sensitivity have been noted and studied previously. We did not set out to establish the details of the molecular determinants of the drug-binding site for each individual subunit. Although the latter issue is of great interest, it goes well beyond the scope of the present study. The S6+C-terminal chimeras containing the S6+C-terminal of Kv3.1 or Kv1.5 moved the flecainide sensitivity toward that of the subunit composition of the S6+C-terminal end. However, despite the fact that the S6+C-terminal contained the leucine/isoleucine moiety conferring flecainide sensitivity/insensitivity, respectively, in the respective WT or point mutations, the changes in drug sensitivity were less with the chimeras than for the point mutations. This observation suggests that other molecular determinants in S6 and/or the C terminus influence drug sensitivity in the chimeras and can partly offset the effects of the leucine/isoleucine moiety.

The channel-blocking concentrations in this study are higher than those produced therapeutically, as well as values published in studies analyzing the effects of flecainide on $I_{Kur,d}$ in isolated atrial cells and in vivo models of atrial fibrillation (Wang et al., 1992; Yue et al., 2000a). This discrepancy is probably a result of the well recognized lesser sensitivity to blocking drugs of channels expressed in *Xenopus laevis* oocytes compared with mammalian cells (Weerapura et al., 2002). Nevertheless, the mechanisms of channel block in *X. laevis* oocytes are believed to be similar to those in other systems, and *X. laevis* oocytes are widely used as an expression system for the analysis of structural motifs for channel block (Dibb et al., 2003; Wang et al., 2003; Decher et al., 2004; Perry et al., 2004).

We used molecular modeling to evaluate the position of the critical leucine/isoleucine amino acid in relationship to key structural components of Kv3.1. We recognize that this modeling does not clarify the details of flecainide binding. As mentioned above, a full evaluation of the molecular structure of the drug-binding site goes beyond the scope of this study. In particular, further work is needed to delineate the amino acids that form the binding site and the mechanism of their interaction with the critical leucine/isoleucine residue that we identified. Nevertheless, we feel that it is important to note the position of the leucine/isoleucine amino acid site to begin to assess potential mechanisms of its involvement. Further work will clearly be needed to reveal more of the details of flecainide's interactions with channels composed of Kv4.2, Kv3.1, Kv1.4, and Kv1.5 subunits.

Acknowledgments

We thank Evelyn Landry and Xiaofan Yang for expert technical assistance and France Thériault for excellent secretarial help with the manuscript.

References

Armstrong CM (1971) Interaction of tetraethylammonium ion derivatives with the potassium channels of giant axons. *J Gen Physiol* **58:**413–437.

Brooks BR, Bruccoleri RE, Olafson BD, States DJ, Swaminathan S, and Karplus M (1983) A program for macromolecular energy minimization and dynamics calculations. *J Comput Chem* **4:**187–217.

Caballero R, Moreno I, Gonzalez T, Valenzuela C, Tamargo J, and Delpon E (2002) Putative binding sites for benzocaine on a human cardiac cloned channel (Kv1.5). *Cardiovasc Res* **56:**104–117.

Caballero R, Pourrier M, Schram G, Delpon E, Tamargo J, and Nattel S (2003) Effects of flecainide and quinidine on Kv4.2 currents: voltage dependence and role of S6 valines. *Br J Pharmacol* **138:**1475–1484.

Decher N, Pirard B, Bundis F, Peukert S, Baringhaus KH, Busch AE, Steinmeyer K, and Sanguinetti MC (2004) Molecular basis for Kv1.5 channel block: conservation of drug binding sites among voltage-gated K^+ channels. *J Biol Chem* **279:**394–400.

Dibb KM, Rose T, Makary SY, Claydon TW, Enkvetchakul D, Leach R, Nichols CG, and Boyett MR (2003) Molecular basis of ion selectivity, block and rectification of the inward rectifier Kir3.1/Kir3.4 K^+ channel. *J Biol Chem* **278:**49537–49548.

Doyle DA, Morais CJ, Pfuetzner RA, Kuo A, Gulbis JM, Cohen SL, Chait BT, and MacKinnon R (1998) The structure of the potassium channel: molecular basis of K^+ conduction and selectivity. *Science (Wash DC)* **280:**69–77.

Fedida D, Eldstrom J, Hesketh JC, Lamorgese M, Castel L, Steele DF, and Van Wagoner DR (2003) Kv1.5 is an important component of repolarizing K^+ current in canine atrial myocytes. *Circ Res* **93:**744–751.

Feng J, Wible B, Li GR, Wang Z, and Nattel S (1997) Antisense oligodeoxynucleotides directed against Kv1.5 mRNA specifically inhibit ultrarapid delayed rectifier K^+ current in cultured adult human atrial myocytes. *Circ Res* **80:**572–579.

Fernandez D, Ghanta A, Kauffman GW, and Sanguinetti MC (2004) Physicochemical features of the HERG channel drug binding site. *J Biol Chem* **279:**10120–10127.

Franqueza L, Longobardo M, Vicente J, Delpon E, Tamkun MM, Tamargo J, Snyders DJ, and Valenzuela C (1997) Molecular determinants of stereoselective bupivacaine block of hKv1.5 channels. *Circ Res* **81:**1053–1064.

Han W, Wang Z, and Nattel S (2000) A comparison of transient outward currents in canine cardiac Purkinje cells and ventricular myocytes. *Am J Physiol* **279:**H466–H474.

Herrera D, Yue L, Wang Z, and Nattel S (2002) Effects of antiarrhythmic drugs on currents carried by dKv3.1 and hKv1.5 (Abstract). *Biophys J* **82:**585a.

Hockerman GH, Johnson BD, Abbott MR, Scheuer T, and Catterall WA (1997) Molecular determinants of high affinity phenylalkylamine block of L- type calcium channels in transmembrane segment IIIS6 and the pore region of the alpha1 subunit. *J Biol Chem* **272:**18759–18765.

Hughey R and Krogh A (1996) Hidden Markov models for sequence analysis: extension and analysis of the basic method. *Comput Appl Biosci* **12:**95–107.

Jiang Y, Lee A, Chen J, Cadene M, Chait BT, and MacKinnon R (2002) The open pore conformation of potassium channels. *Nature (Lond)* **417:**523–526.

Judge SI, Yeh JZ, Goolsby JE, Monteiro MJ, and Bever CT Jr (2002) Determinants of 4-aminopyridine sensitivity in a human brain Kv1.4 K^+ channel: phenylalanine substitutions in leucine heptad repeat region stabilize channel closed state. *Mol Pharmacol* **61:**913–920.

Laskowski BR, MacArthur MW, Moss DS, and Thornton JM (1993) PROCHECK: A program to check the stereochemical quality of protein structures. *J Appl Cryst* **26:**283–291.

Lees-Miller JP, Duan Y, Teng GQ, and Duff HJ (2000) Molecular determinant of high-affinity dofetilide binding to HERG1 expressed in *Xenopus* oocytes: involvement of S6 sites. *Mol Pharmacol* **57:**367–374.

Liu Y, Holmgren M, Jurman ME, and Yellen G (1997) Gated access to the pore of a voltage-dependent K^+ channel. *Neuron* **19:**175–184.

Mitcheson JS, Chen J, Lin M, Culberson C, and Sanguinetti MC (2000) A structural basis for drug-induced long QT syndrome. *Proc Natl Acad Sci USA* **97:**12329–12333.

Nattel S, Khairy P, Roy D, Thibault B, Guerra P, Talajic M, and Dubuc M (2002) New approaches to atrial fibrillation management: a critical review of a rapidly evolving field. *Drugs* **62:**2377–2397.

Nattel S, Yue L, and Wang Z (1999) Cardiac ultrarapid delayed rectifiers, a novel potassium current family of functional similarity and molecular diversity. *Cell Physiol Biochem* **9:**217–226.

Perry M, de Groot MJ, Helliwell R, Leishman D, Tristani-Firouzi M, Sanguinetti MC, and Mitcheson J (2004) Structural determinants of HERG channel block by clofilium and ibutilide. *Mol Pharmacol* **66:**240–249.

Ragsdale DS, McPhee JC, Scheuer T, and Catterall WA (1996) Common molecular determinants of local anesthetic, antiarrhythmic and anticonvulsant block of voltage-gated Na^+ channels. *Proc Natl Acad Sci USA* **93:**9270–9275.

Roden DM and George AL Jr (1997) Structure and function of cardiac sodium and potassium channels. *Am J Physiol* **273:**H511–H525.

Sali A and Blundell TL (1993) Comparative protein modelling by satisfaction of spatial restraints. *J Mol Biol* **234:**779–815.

Seebohm G, Chen J, Strutz N, Culberson C, Lerche C, and Sanguinetti MC (2003) Molecular determinants of KCNQ1 channel block by a benzodiazepine. *Mol Pharmacol* **64:**70–77.

Snyders DJ (1999) Structure and function of cardiac potassium channels. *Cardiovasc Res* **42:**377–390.
Sunami A, Dudley SC Jr, and Fozzard HA (1997) Sodium channel selectivity filter regulates antiarrhythmic drug binding. *Proc Natl Acad Sci USA* **94:**14126–14131.
Tamargo J, Caballero R, Gomez R, Valenzuela C, and Delpon E (2004) Pharmacology of cardiac potassium channels. *Cardiovasc Res* **62:**9–33.
Varro A, Biliczki P, Iost N, Virag L, Hala O, Kovacs P, Matyus P, and Papp JG (2004) Theoretical possibilities for the development of novel antiarrhythmic drugs. *Curr Med Chem* **11:**1–11.
Wang S, Morales MJ, Qu YJ, Bett GC, Strauss HC, and Rasmusson RL (2003) Kv1.4 channel block by quinidine: evidence for a drug-induced allosteric effect. *J Physiol* **546:**387–401.
Wang Z, Fermini B, and Nattel S (1993) Sustained depolarization-induced outward current in human atrial myocytes. Evidence for a novel delayed rectifier K^+ current similar to Kv1.5 cloned channel currents. *Circ Res* **73:**1061–1076.
Wang Z, Fermini B, and Nattel S (1995) Effects of flecainide, quinidine and 4-aminopyridine on transient outward and ultrarapid delayed rectifier currents in human atrial myocytes. *J Pharmacol Exp Ther* **272:**184–196.
Wang Z, Pagé P, and Nattel S (1992) Mecahnism of flecainide's antiarrhythmic action in experimental atrial fibrillation. *Circ Res* **71:**271–287.
Weerapura M, Nattel S, Chartier D, Caballero R, and Hébert TE (2002) A comparison of currents carried by HERG, with and without coexpression of MiRP1 and the native rapid delayed rectifier current. Is MiRP1 the missing link? *J Physiol (Lond)* **540:**15–27.
Weiner SJ, Kollman PA, Case DA, Singh UC, Ghio C, Alagona G, Profeta S, and Weiner P (1984) A new force field for molecular mechanical simulation of nucleic acids and proteins. *J Am Chem Soc* **106:**765–784.
Wulff H, Gutman GA, Cahalan MD, and Chandy KG (2001) Delineation of the clotimazol/TRAM-34 binding site on the intermediate conductance calcium activated potassium channel, IKCa1. *J Biol Chem* **276:**30240–30245.
Yamagishi T, Ishii K, and Taira N (1995) Antiarrhythmic and bradycardic drugs inhibit currents of cloned K^+ channels, Kv1.2 and Kv1.4. *Eur J Pharmacol* **281:** 151–159.
Yeola SW, Rich TC, Uebele VN, Tamkun MM, and Snyders DJ (1996) Molecular analysis of a binding site for quinidine in a human cardiac delayed rectifier K^+ channel. Role of S6 in antiarrhythmic drug binding. *Circ Res* **78:**1105–1114.
Yeola SW and Snyders DJ (1997) Electrophysiological and pharmacological correspondence between Kv4.2 current and rat cardiac transient outward current. *Cardiovasc Res* **33:**540–547.
Yue L, Feng J, Li GR, and Nattel S (1996) Characterization of an ultrarapid delayed rectifier potassium channel involved in canine atrial repolarization. *J Physiol (Lond)* **496:**647–662.
Yue L, Feng JL, Wang Z, and Nattel S (2000a) Effects of ambasilide, quinidine, flecainide and verapamil on ultra-rapid delayed rectifier potassium currents in canine atrial myocytes. *Cardiovasc Res* **46:**151–161.
Yue L, Wang Z, Rindt H, and Nattel S (2000b) Molecular evidence for a role of Shaw (Kv3) potassium channel subunits in potassium currents of dog atrium. *J Physiol* **527:**467–478.
Zhang H, Zhu B, Yao JA, and Tseng GN (1998) Differential effects of S6 mutations on binding of quinidine and 4-aminopyridine to rat isoform of Kv1.4: common site but different factors in determining blockers' binding affinity. *J Pharmacol Exp Ther* **287:**332–343.
Zhang S, Zhou Z, Gong Q, Makielski JC, and January CT (1999) Mechanism of block and identification of the verapamil binding domain to HERG potassium channels. *Circ Res* **84:**989–998.

Address correspondence to: Dr. Stanley Nattel, Research Center, Montreal Heart Institute, 5000 Belanger St E, Montreal, Quebec, Canada, H1T 1C8. E-mail: stanley.nattel@icm-mhi.org